HHS Public Access

Author manuscript

Magn Reson Imaging. Author manuscript; available in PMC 2020 June 01.

Published in final edited form as:

Magn Reson Imaging. 2019 June ; 59: 46–52. doi:10.1016/j.mri.2019.03.003.

Evaluation of cerebrovascular reserve in patients with cerebrovascular diseases using resting-state MRI: a feasibility study

Kamil Taneja[a], **Hanzhang Lu**[a,b], **Babu G. Welch**[c,d], **Binu Thomas**[e], **Marco Pinho**[d], **Doris Lin**[a], **Argye E. Hillis**[f], and **Peiying Liu**[a]

[a]The Russell H. Morgan Department of Radiology & Radiological Science, Johns Hopkins University School of Medicine, Baltimore, MD 21287

[b]F.M. Kirby Center for Functional Brain Imaging, Kennedy Krieger Institute, Baltimore, MD 21205

[c]Department of Neurological Surgery, UT Southwestern Medical Center, Dallas, TX 75390, USA

[d]Department of Radiology, UT Southwestern Medical Center, Dallas, TX 75390, USA

[e]Advanced Imaging Research Center, University of Texas Southwestern Medical Center, Dallas, TX, USA.

[f]Department of Neurology, Johns Hopkins University School of Medicine, Baltimore, MD 21287

Abstract

Purpose: To demonstrate the feasibility of mapping cerebrovascular reactivity (CVR) using resting-state functional MRI (fMRI) data without gas or other challenges in patients with cerebrovascular diseases and to show that brain regions affected by the diseases have diminished vascular reactivity.

Materials and Methods: Two sub-studies were performed on patients with stroke and Moyamoya disease. In Study 1, 20 stroke patients (56.3±9.7 years, 7 females) were enrolled and resting-state blood-oxygenation-level-dependent (rs-BOLD) fMRI data were collected, from which CVR maps were computed. CVR values were compared across lesion, perilesional and control ROIs defined on anatomic images. Reproducibility of the CVR measurement was tested in 6 patients with follow-up scans. In Study 2, rs-BOLD fMRI and dynamic susceptibility contrast (DSC) MRI scans were collected in 5 patients with Moyamoya disease (32.4±8.2 years, 4 females). Cerebral blood flow (CBF), cerebral blood volume (CBV), and time-to-peak (TTP) maps were obtained from the DSC MRI data. CVR values were compared between stenotic brain regions and control regions perfused by non-stenotic arteries.

Corresponding author: Peiying Liu, Ph.D., The Russell H. Morgan Department of Radiology & Radiological Science, Johns Hopkins University School of Medicine, 600 N. Wolfe Street, Park 324, Baltimore, MD 21287, peiying.liu@jhu.edu.

Results: In stroke patients, lesion CVR (0.250 ± 0.055 relative unit (r.u.)) was lower than control CVR (0.731±0.088 r.u., p=0.0002). CVR was also lower in the perilesional regions in a graded manner (perilesion 1 CVR = 0.422±0.051 r.u., perilesion 2 CVR = 0.492±0.046 r.u.), relative to that in the control regions (p = 0.005 and 0.036, respectively). In the repeatability analysis, a strong correlation was observed between lesion CVR (r^2=0.91, p=0.006) measured at two time points, as well as between control CVR (r^2=0.79, p=0.036) at two time points. In Moyamoya patients, CVR in the perfusion deficit regions delineated by DSC TTP maps (0.178±0.189 r.u.) was lower than that in the control regions (0.868±0.214 r.u., p=0.013). Furthermore, the extent of reduction in CVR was significantly correlated with the extent of lengthening in TTP (r^2=0.91, p=0.033).

Conclusion: Our findings suggested that rs-BOLD data can be used to reproducibly evaluate CVR in patients with cerebrovascular diseases without the use of any vasoactive challenges.

Keywords

Cerebrovascular Reactivity; Resting-State; BOLD; stroke; Moyamoya disease; time-to-peak

1. Introduction

Cerebrovascular reactivity (CVR), as an index of cerebrovascular reserve, provides valuable information in the diagnosis and treatment evaluation of patients with various cerebrovascular diseases [1-9]. Diminished CVR is a risk factor of stroke in patients with arterial stenosis [1, 8, 9], and is also thought to be associated with the risk of future infarct in patients with acute ischemic stroke (AIS) [10]. Therefore, evaluation of CVR has important clinical value in the diagnosis and management of cerebrovascular diseases, especially in arterial stenosis and stroke.

Currently, assessment of CVR requires the administration of a vasoactive challenge, e.g. injection of acetazolamide (ACZ), inhalation of carbon dioxide (CO2), or breath-holding, while monitoring cerebral perfusion responses using MRI, CT, or SPECT [9, 11-15]. However, application of such vasoactive challenges is often difficult or impractical to patients such as AIS patients. Although there have been reports on CVR in subacute (1 day to 2 weeks) and chronic (>2 weeks) patients after stroke using breath-holding [16, 17], to our knowledge, there have not been MRI studies evaluating CVR in acute (<24 hours) stroke patients due to a lack of practical tools. Even for chronic patients, the complex procedure, added time, and costs often result in CVR imaging being substantially under-utilized in clinical settings.

The purpose of the present study is to demonstrate the feasibility of mapping CVR without using any physiological challenges in clinical populations. The technique exploits resting-state (rs) blood-oxygenation-dependent-level (BOLD) fluctuations due to natural fluctuations in breathing pattern and was originally demonstrated and validated in healthy volunteers [18]. In the present work, two clinical populations were tested. First, in stroke patients, we evaluated rs-CVR in brain regions corresponding to stroke lesion, perilesional area, and contralateral normal tissues. In a sub-group of the patients, we repeated the rs-BOLD scan in a follow-up visit and reproducibility between the original and follow-up rs-

CVR results was examined. Second, in patients with Moyamoya disease, which is a steno-occlusive cerebrovascular disease, we evaluated rs-CVR in stenotic and normal brain regions, and compared the rs-CVR measures to the time-to-peak (TTP) measures obtained using dynamic susceptibility contrast (DSC) MRI. We hypothesize that CVR measured by rs-BOLD is sensitive and reliable in detecting vascular deficit in stroke and Moyamoya disease.

2. Materials and Methods

2.1 Study in stroke patients

Subjects included in this study were part of a larger stroke study enrolled between 2012 and 2016 [19-22]. The study was approved by the Institutional Review Board of the Johns Hopkins University School of Medicine, and the data was obtained with written consent. The subject selection criteria were: (a) must have a clinically confirmed stroke within 16 months prior to the MRI scan; (b) must have a rs-BOLD scan; (c) have at least a T2-weighted image or diffusion-weighted image (DWI) in the same session of the rs-BOLD scan. Of the 68 subjects available in the larger study, 20 subjects (56.3±9.7 years, 7 females) met the criteria. Their demographic and clinical information are listed in Table 1. In six patients, the rs-BOLD scan was repeated in a follow-up visit, which allowed us to test the reproducibility of the rs-CVR measure.

All scans were performed on 3T MRI systems (Philips Healthcare, Best, The Netherlands, and Siemens Healthineers, Erlangen, Germany). The rs-BOLD scan was performed while the subject was asked to lie still and open their eyes in the MRI scanner without performing any task. The following imaging parameters were used: Field-of-view (FoV)=240×240×140mm^3, TR=2000ms, TE=30ms, flip angle=75°, matrix size=80×80×35, resolution=3×3×4mm^3, 210 image volumes, scan duration 7 min 12 sec. T2-weighted MRI used the following parameters: FoV=212×212×154mm^3, TR=4200ms, TE=12ms, resolution=0.8×0.8×2.2mm^3, scan duration 3 min 28 sec. The DWI imaging parameters were: FoV=212×212×154mm^3, TR=7000ms, TE=71ms, thirty-three gradient orientations with b=700 s/mm^2, resolution=0.8×0.8×2.2mm^3, scan duration 4 min 35 sec.

2.2 Study in Moyamoya patients

Five patients with Moyamoya disease (32.4±8.2 years, 4 females) were recruited in this sub-study. These patients were characterized by severe narrowing/blockage of the anterior and middle cerebral vessels. The specific diagnosis of each patient in this study is listed in Table 2. The study protocol was approved by the Institutional Review Boards of the Johns Hopkins University School of Medicine and University of Texas Southwestern Medical Center. Written informed consent was obtained from all participants before the study.

The MRI scans were performed on 3T MRI systems (Philips Healthcare, Best, The Netherlands). The imaging parameters of the rs-BOLD scan were: Field-of-view (FoV)=205×205×150mm^3, TR=1510ms, TE=21ms, flip angle=90°, matrix size=64×64×36, 3.2 mm isotropic voxels, whole brain coverage using 36 slices with 1mm gap, 372 image volumes, scan duration 9 min 20 sec. Anatomical images of T2-FLAIR (1.07×1.07×1.1 mm^3

resolution), T1-weighted MPRAGE (1 mm^3 resolution), and time-of-flight (TOF) angiogram were also obtained. A DSC scan was performed at the end the MRI session: Gadolinium contrast agent (Gadavist, Bayer Healthcare), dosage 0.1 mmol/kg, injection rate: 5 ml/s, identical imaging parameters as the rs-BOLD scan, duration=1.26 min. Cerebral blood flow (CBF), cerebral blood volume (CBV), and time-to-peak (TTP) maps were obtained from the DSC data using FDA-approved, vendor-provided processing tool.

2.3 Data Processing

Data analysis was performed using Statistical Parametric Mapping (University College London, UK) and in-house MATLAB (MathWorks, Natick, MA) scripts. Figure 1 shows a flow chart of the processing pipeline, which is similar to procedures established in a prior study in healthy subjects [18]. Rs-BOLD images first underwent pre-processing steps including motion correction, spatial smoothing with a Gaussian filter with a full-width-half-maximum (FWHM) of 4mm, and linear detrending. Next, based on the previous findings in healthy volunteers that global rs-BOLD fluctuations within 0.02 to 0.04 Hz are mostly attributed to natural fluctuations in end-tidal (Et) CO2 levels [18], we temporally filtered the rs-BOLD data with a band-pass filter of 0.02 to 0.04 Hz. For stroke patients, a whole-brain mask was applied on the rs-BOLD images to obtain an average whole-brain rs-BOLD time course, which was used as a reference signal. For Moyamoya patients, cerebellum gray matter mask extracted from T1-MPRAGE image was used as the reference mask because posterior circulation is least affected in Moyamoya patients. A general linear model was employed on a voxel-by-voxel basis with the reference rs-BOLD signal as the independent variable and the voxel's signal time course as the dependent variable, yielding a CVR index in % signal change. Since we were primarily interested in within-subject comparisons between disease-affected and other brain regions, the CVR index was normalized to the reference region values, yielding a relative CVR map. The relative CVR maps were then coregistered to the DWI or T2-weighted anatomic images where ROIs were defined.

To quantify CVR in different brain areas in stroke patients, regions-of-interest (ROIs) of lesion and control regions were manually delineated on structural images by a rater blinded to the CVR map. The manually delineated ROIs were reviewed and confirmed by a neuroradiologist. DWI was used for ROI drawing in acute/subacute patients (0 week, N=5) due to its higher sensitivity to lesions at this stage. T2-weighted image was used for ROI drawing in more chronic patients (≥1 weeks, N=15), except in two patients (1 week and 32 weeks, respectively) who only had DWI available. ROIs corresponding to stroke lesions (hyperintense areas) were drawn on up to 5 consecutive axial slices, when present. Control ROIs were defined as the mirrored-location on the contralateral healthy side. Additionally, two perilesional ROIs were defined. Perilesional ROI 1 (P1) was defined by dilating the lesion ROI with one layer of voxels three-dimensionally for four times. Perilesional ROI 2 (P2) was defined by further dilating the P1 four times. All ROIs were mutually exclusive. Then, ROIs were applied to the coregistered CVR maps to obtain average CVR in each ROIs. In the patients who received a follow-up rs-BOLD scan, the ROIs of the original time point were applied to the CVR map of the follow-up data, after coregistering the follow-up images to the original time point.

For the Moyamoya study data, CBF, CBV and TTP maps were first coregistered to the rs-BOLD scan, and then transformed to MNI space together with the rs-CVR maps via T1-MPRAGE. For each patient, an ROI of perfusion deficit area was manually delineated as regions with prolonged TTP values on 5 consecutive axial slices of the TTP map, by a rater blinded to the CVR map. The control ROI was generated based on the posterior cerebral artery (PCA) territory from a perfusion atlas that has been reported previously [23], on the same axial slices of the stenotic ROI. Note that the control ROIs in the Moyamoya study were not defined based on mirrored locations because many Moyamoya patients have bilateral stenosis. Averaged CVR within each ROI was obtained.

2.4 Statistical Analysis

All CVR results are reported in mean ± standard error. For data from the stroke study, one-way ANOVA with repeated measurements was performed to compare CVR among the four ROIs. Post-hoc paired t-tests were performed to compare CVR between each pair of ROIs. For patients who received the follow-up rs-BOLD scan, CVR between the initial and follow-up data were compared using cross-correlation and paired t-tests. For data from the Moyamoya study, paired t-test was performed to compare CVR between stenotic and control ROIs. In stenotic ROIs, regression analysis was further performed to evaluate the association between reduction in CVR ($CVR_{stenotic}/CVR_{control}$) and lengthening in TTP ($TTP_{stenotic}$-$TTP_{control}$). In all analyses, a p value (with Bonferroni correction when applicable) of 0.05 or less was considered significant.

3. Results

3.1. Stroke study

CVR maps of four representative stroke patients are shown in Figure 2. Typical ROIs are also displayed. Figure 3 summarizes CVR values in ROIs corresponding to stroke lesions (0.250 ± 0.055 relative unit (r.u.)), perilesional ROI 1 (0.422 ± 0.051 r.u.), perilesional ROI 2 (0.492 ± 0.046 r.u.), and contralateral control region (0.731 ± 0.088 r.u.). ANOVA analysis revealed a significant difference in CVR across ROIs ($p<0.001$). Post-hoc analysis showed that CVR was different (corrected $p<0.04$) between each pairs of the ROIs. Stroke lesions manifested a lower CVR compared to perilesional regions, which are in turn lower than control regions. This observation was also found in the subgroups of acute patients (0 week, N=5) and chronic patients (N=15) separately. Relative to control regions, CVR in stroke lesions were diminished by 62.8±7.2%.

In the six patients who had a follow-up visit, the NIHSS score was 1.67±1.03 at the initial visit and 1.17±0.75 at the follow-up visit, with no significant differences between the visits ($p=0.18$). No new lesions were found on their structural images. A strong correlation ($r2=0.91$, $p=0.006$) was observed between CVR in the stroke lesions during the initial visit and that measured during the follow-up visit (time gap = 24.7±13.3 weeks), suggesting an excellent reproducibility of the proposed CVR technique. A similar ($r2=0.79$, $p=0.036$) was observed for CVR in the control regions. No significant difference was found between the correlation coefficient in the stroke lesions and that in the control regions ($p=0.59$). Due to

the small sample in the follow-up data, we did not investigate the time-dependent changes in CVR in the present study.

3.2. Moyamoya study

CVR maps of all five Moyamoya patients are shown in Figure 4. For reference, maximum-intensity-projection (MIP) images of the patients' TOF-MRA are also shown, illustrating the specific stenosis site of each patient (red arrows). FLAIR, CBF, CBV and TTP maps are also displayed. Prolonged TTP and reduced CVR are the most evident observations in these images. On the other hand, FLAIR, CBF and CBV show fewer abnormalities.

Results of the ROI analysis are summarized in Figure 5. As shown in Figure 5a, stenotic CVR (0.178±0.189 r.u.) was significantly lower than control CVR (0.868±0.214 r.u., $p=0.013$). In the stenotic brain regions, reduction in CVR is significantly correlated with lengthening in TTP ($r^2=0.91$, $p=0.033$).

4. Discussion

In this study, we demonstrated the initial feasibility of CVR evaluation in patients with stroke and Moyamoya disease using rs-BOLD MRI without needing any physiological challenge or contrast agent. Our results suggested that the CVR maps obtained from the rs-BOLD data is sensitive in detecting disease-related reduction in cerebrovascular reserve in these patients. We also showed that this CVR mapping method is reproducible, and its result is in good agreement with the DSC-TTP result.

Mapping of CVR in the brain traditionally requires an explicit physiological maneuver, such as acetazolamide injection [9, 11, 24], breath-holding [16, 25-30], inhalation of CO2 [4, 31-35], or hyperventilation [7, 36]. However, in patient populations, these methods often encounter practical difficulties. Thus these techniques have not been widely used in cerebrovascular diseases. For example, CO2 inhalation requires special apparatus and involves mouthpiece or facemask [32, 34, 37, 38]. Breath-holding or hyperventilation requires considerable patient cooperation [27]. The scan time for an acetazolamide challenge is usually long in order to allow the pharmacological agent to take effect [39]. The present study exploits natural variations in breathing pattern to extract CVR from the rs-BOLD data. When dividing rs-BOLD fluctuations into different frequency segments and examine their correspondence to end-tidal CO2 recorded during the experiment, it was previously found that a frequency range of 0.02-0.04 Hz contains the most prominent effects from CO2 fluctuations [18]. Therefore, the present study used the bandpass-filtered global BOLD time-course as the regressor in CVR computation. The rs-CVR technique can be performed either with or without simultaneous recording of end-tidal CO2 (Et-CO2) time course. In the absence of CO2 recording as applied in this work, this approach does not provide an absolute CVR in units of % signal per mmHg CO2, but is expected to be sufficient in stroke and intracranial stenosis studies that usually compare disease-affected regions to healthy regions. It should also be noted that rs-CVR method has been directly validated with CO2-based CVR in healthy controls [18]. The spatial correlation between rs-CVR and CO2-based CVR was 0.88 in healthy controls, which was similar to the intra-subject correlations of rs-CVR maps (0.91) [18] and CO2-based CVR maps (0.93) [40].

Our results indicate that stroke lesions have a CVR deficit, in agreement with previous studies [11, 41, 42]. We also noted that CVR increases distally from lesion to perilesional regions, confirming that the exhaustion of reactivity is most severe in the stroke core [43-45]. Compared to contralateral control regions, perilesional regions also revealed a reduced CVR. This may be because blood vessels in these regions are already dilated to preserve CBF in the presence of reduced perfusion pressure. Thus, these may be regions with a loss of vascular reserve and a higher risk to develop hemodynamic failure [46, 47]. These findings support the use of resting-state CVR as a biomarker for delineation of high-risk tissues in ischemic cerebrovascular diseases. Although CVR reduction would be associated with CBF reduction in the acute phase after stroke, since CVR can detect such stroke-affected tissue with vascular compromise before CBF change can be observed, the use of CVR-diffusion mismatch can potentially provide a more sensitive tool for delineation of penumbra tissue in acute ischemic stroke management. CVR may also have a relationship with apparent diffusion coefficient (ADC) which has been found to decrease in acute and subacute stroke patient [48, 49], as vascular dysfunction indicated by lower CVR can cause tissue ischemia that restricts diffusion and results in a lower ADC.

Diminished CVR shown in our results in Moyamoya disease are also in agreement with previous literature using CO_2 gas inhalation methods [4, 5, 50]. In addition to the dampened cerebrovascular reserve, our results further revealed an association between the degree of CVR deficit and delayed TTP. Delayed TTP has been suggested to be an important biomarker in many cerebrovascular diseases [51-53]. Therefore, rs-CVR obtained from rs-BOLD data may be a useful alternative of TTP in cerebrovascular diseases when DSC contrast injection and CO_2 gas inhalation are not applicable in patients.

There are some limitations in this study. First, the selection of frequency band of 0.02-0.04 Hz in the BOLD signal was based on empirical observations in healthy volunteers from a previous study [18], which found that this frequency range provided the highest correlation with the end-tidal CO_2 time-courses. However, it is possible that such band-pass filtered signals still contain some contributions from other signal sources, such as motion and cardiac pulsatility. For stroke patients with different cardiac pulsatility, the optimal frequency band of the band-pass filter needs to be verified. Another limitation is that this study is meant to be a proof-of-principle of the clinical feasibility of a novel MRI technique, and the stroke patients recruited ranged from subacute to chronic stage and the sample size of the Moyamoya patients was also limited. Nonetheless, the significance of the present work is that it serves to provide a foundation for future larger scale studies of stroke and Moyamoya patients.

5. Conclusions

CVR imaging based on resting-state BOLD MRI provides a task-free and reproducible method to measure vascular reserve in stroke and Moyamoya patients. This technique can reveal hemodynamic failure of the disease-affected regions, and may be a useful biomarker in cerebrovascular diseases.

Acknowledgments

Funding

This work was supported by the National Institutes of Health [grant numbers R01DC005375 (to A.H.), NIH P50 DC014664 (to A.H.), NIH R01 NS106702 (to H.L.), NIH R01 MH084021 (to H.L.), NIH R01 AG047972 (to H.L.), NIH R01 NS106711 (to H.L.), NIH R21 NS095342 (to H.L.), NIH R21 NS100006 (to P.L.), and NIH P41 EB015909 (to H.L.)] and American Heart Association [grant number AHA 17GRNT33411174 (to P.L.)].

References

[1]. Gupta A, Chazen JL, Hartman M, Delgado D, Anumula N, Shao H, et al. Cerebrovascular reserve and stroke risk in patients with carotid stenosis or occlusion: a systematic review and meta-analysis. Stroke 2012;43(11):2884–91. [PubMed: 23091119]

[2]. Mandell DM, Han JS, Poublanc J, Crawley AP, Stainsby JA, Fisher JA, et al. Mapping cerebrovascular reactivity using blood oxygen level-dependent MRI in Patients with arterial steno-occlusive disease: comparison with arterial spin labeling MRI. Stroke 2008;39(7):2021–8. [PubMed: 18451352]

[3]. De Vis JB, Petersen ET, Bhogal A, Hartkamp NS, Klijn CJ, Kappelle LJ, et al. Calibrated MRI to evaluate cerebral hemodynamics in patients with an internal carotid artery occlusion. Journal of cerebral blood flow and metabolism : official journal of the International Society of Cerebral Blood Flow and Metabolism 2015;35(6):1015–23.

[4]. Donahue MJ, Ayad M, Moore R, van Osch M, Singer R, Clemmons P, et al. Relationships between hypercarbic reactivity, cerebral blood flow, and arterial circulation times in patients with moyamoya disease. Journal of magnetic resonance imaging : JMRI 2013;38(5):1129–39. [PubMed: 23440909]

[5]. Mikulis DJ, Krolczyk G, Desal H, Logan W, Deveber G, Dirks P, et al. Preoperative and postoperative mapping of cerebrovascular reactivity in moyamoya disease by using blood oxygen level-dependent magnetic resonance imaging. Journal of neurosurgery 2005;103(2):347–55. [PubMed: 16175867]

[6]. Marstrand JR, Garde E, Rostrup E, Ring P, Rosenbaum S, Mortensen EL, et al. Cerebral perfusion and cerebrovascular reactivity are reduced in white matter hyperintensities. Stroke 2002;33(4): 972–6. [PubMed: 11935046]

[7]. Krainik A, Hund-Georgiadis M, Zysset S, von Cramon DY. Regional impairment of cerebrovascular reactivity and BOLD signal in adults after stroke. Stroke 2005;36(6):1146–52. [PubMed: 15879326]

[8]. Reinhard M, Schwarzer G, Briel M, Altamura C, Palazzo P, King A, et al. Cerebrovascular reactivity predicts stroke in high-grade carotid artery disease. Neurology 2014;83(16):1424–31. [PubMed: 25217057]

[9]. Yonas H, Smith HA, Durham SR, Pentheny SL, Johnson DW. Increased stroke risk predicted by compromised cerebral blood flow reactivity. Journal of neurosurgery 1993;79(4):483–9. [PubMed: 8410214]

[10]. Zaharchuk G Arterial spin label imaging of acute ischemic stroke and transient ischemic attack. Neuroimaging clinics of North America 2011;21(2):285–301, x. [PubMed: 21640300]

[11]. Ogasawara K, Ogawa A, Yoshimoto T. Cerebrovascular reactivity to acetazolamide and outcome in patients with symptomatic internal carotid or middle cerebral artery occlusion: a xenon-133 single-photon emission computed tomography study. Stroke 2002;33(7):1857–62. [PubMed: 12105366]

[12]. Liu P, De Vis JB, Lu H. Cerebrovascular reactivity (CVR) MRI with CO2 challenge: A technical review. NeuroImage 2018.

[13]. Settakis G, Molnár C, Kerényi L, Kollár J, Legemate D, Csiba L, et al. Acetazolamide as a vasodilatory stimulus in cerebrovascular diseases and in conditions affecting the cerebral vasculature. European Journal of Neurology 2003;10(6):609–20. [PubMed: 14641504]

[14]. Marshall O, Lu H, Brisset JC, Xu F, Liu P, Herbert J, et al. Impaired cerebrovascular reactivity in multiple sclerosis. JAMA neurology 2014;71(10):1275–81. [PubMed: 25133874]

[15]. Peng SL, Chen X, Li Y, Rodrigue KM, Park DC, Lu H. Age-related changes in cerebrovascular reactivity and their relationship to cognition: A four-year longitudinal study. NeuroImage 2018;174:257–62. [PubMed: 29567504]

[16]. Geranmayeh F, Wise RJ, Leech R, Murphy K. Measuring vascular reactivity with breath-holds after stroke: a method to aid interpretation of group-level BOLD signal changes in longitudinal fMRI studies. Human brain mapping 2015;36(5):1755–71. [PubMed: 25727648]

[17]. Raut RV, Nair VA, Sattin JA, Prabhakaran V. Hypercapnic evaluation of vascular reactivity in healthy aging and acute stroke via functional MRI. NeuroImage Clinical 2016;12:173–9. [PubMed: 27437178]

[18]. Liu P, Li Y, Pinho M, Park DC, Welch BG, Lu H. Cerebrovascular reactivity mapping without gas challenges. NeuroImage 2017;146:320–6. [PubMed: 27888058]

[19]. Sebastian R, Long C, Purcell JJ, Faria AV, Lindquist M, Jarso S, et al. Imaging network level language recovery after left PCA stroke. Restorative neurology and neuroscience 2016;34(4): 473–89. [PubMed: 27176918]

[20]. Leigh R, Oishi K, Hsu J, Lindquist M, Gottesman RF, Jarso S, et al. Acute lesions that impair affective empathy. Brain : a journal of neurology 2013;136(Pt 8):2539–49. [PubMed: 23824490]

[21]. Purcell J, Sebastian R, Leigh R, Jarso S, Davis C, Posner J, et al. Recovery of orthographic processing after stroke: A longitudinal fMRI study. Cortex; a journal devoted to the study of the nervous system and behavior 2017;92:103–18. [PubMed: 28463704]

[22]. Jarso S, Li M, Faria A, Davis C, Leigh R, Sebastian R, et al. Distinct mechanisms and timing of language recovery after stroke. Cognitive neuropsychology 2013;30(7-8):454–75. [PubMed: 24472056]

[23]. van Laar PJ, Hendrikse J, Golay X, Lu H, van Osch MJ, van der Grond J. In vivo flow territory mapping of major brain feeding arteries. NeuroImage 2006;29(1): 136–44. [PubMed: 16095923]

[24]. Ma J, Mehrkens JH, Holtmannspoetter M, Linke R, Schmid-Elsaesser R, Steiger HJ, et al. Perfusion MRI before and after acetazolamide administration for assessment of cerebrovascular reserve capacity in patients with symptomatic internal carotid artery (ICA) occlusion: comparison with 99mTc-ECD SPECT. Neuroradiology 2007;49(4):317–26. [PubMed: 17200864]

[25]. Chan ST, Evans KC, Rosen BR, Song TY, Kwong KK. A case study of magnetic resonance imaging of cerebrovascular reactivity: a powerful imaging marker for mild traumatic brain injury. Brain Inj 2015;29(3):403–7. [PubMed: 25384127]

[26]. de Boorder MJ, Hendrikse J, van der Grond J. Phase-contrast magnetic resonance imaging measurements of cerebral autoregulation with a breath-hold challenge: a feasibility study. Stroke 2004;35(6):1350–4. [PubMed: 15131315]

[27]. Magon S, Basso G, Farace P, Ricciardi GK, Beltramello A, Sbarbati A. Reproducibility of BOLD signal change induced by breath holding. NeuroImage 2009;45(3):702–12. [PubMed: 19211035]

[28]. Tancredi FB, Hoge RD. Comparison of cerebral vascular reactivity measures obtained using breath-holding and CO2 inhalation. Journal of cerebral blood flow and metabolism : official journal of the International Society of Cerebral Blood Flow and Metabolism 2013;33(7):1066–74.

[29]. Zaca D, Jovicich J, Nadar SR, Voyvodic JT, Pillai JJ. Cerebrovascular reactivity mapping in patients with low grade gliomas undergoing presurgical sensorimotor mapping with BOLD fMRI. Journal of magnetic resonance imaging : JMRI 2014;40(2):383–90. [PubMed: 24338845]

[30]. Bright MG, Murphy K. Reliable quantification of BOLD fMRI cerebrovascular reactivity despite poor breath-hold performance. NeuroImage 2013;83:559–68. [PubMed: 23845426]

[31]. Yezhuvath US, Lewis-Amezcua K, Varghese R, Xiao G, Lu H. On the assessment of cerebrovascular reactivity using hypercapnia BOLD MRI. NMR in biomedicine 2009;22(7):779–86. [PubMed: 19388006]

[32]. Spano VR, Mandell DM, Poublanc J, Sam K, Battisti-Charbonney A, Pucci O, et al. CO2 blood oxygen level-dependent MR mapping of cerebrovascular reserve in a clinical population: safety, tolerability, and technical feasibility. Radiology 2013;266(2):592–8. [PubMed: 23204541]

[33]. De Vis JB, Hendrikse J, Bhogal A, Adams A, Kappelle LJ, Petersen ET. Age-related changes in brain hemodynamics; A calibrated MRI study. Human brain mapping 2015;36(10):3973–87. [PubMed: 26177724]

[34]. Wise RG, Pattinson KT, Bulte DP, Chiarelli PA, Mayhew SD, Balanos GM, et al. Dynamic forcing of end-tidal carbon dioxide and oxygen applied to functional magnetic resonance imaging. Journal of cerebral blood flow and metabolism : official journal of the International Society of Cerebral Blood Flow and Metabolism 2007;27(8):1521–32.

[35]. Amyot F, Kenney K, Moore C, Haber M, Turtzo LC, Shenouda C, et al. Imaging of Cerebrovascular Function in Chronic Traumatic Brain Injury. Journal of neurotrauma 2018;35(10):1116–23. [PubMed: 29065769]

[36]. Bright MG, Bulte DP, Jezzard P, Duyn JH. Characterization of regional heterogeneity in cerebrovascular reactivity dynamics using novel hypocapnia task and BOLD fMRI. Neuroimage 2009;48(1):166–75. [PubMed: 19450694]

[37]. Lu H, Liu P, Yezhuvath U, Cheng Y, Marshall O, Ge Y. MRI mapping of cerebrovascular reactivity via gas inhalation challenges. Journal of visualized experiments : JoVE 2014(94).

[38]. Tancredi FB, Lajoie I, Hoge RD. A simple breathing circuit allowing precise control of inspiratory gases for experimental respiratory manipulations. BMC research notes 2014;7:235. [PubMed: 24725848]

[39]. Hartkamp NS, Hendrikse J, van der Worp HB, de Borst GJ, Bokkers RP. Time course of vascular reactivity using repeated phase-contrast MR angiography in patients with carotid artery stenosis. Stroke 2012;43(2):553–6. [PubMed: 22052518]

[40]. Ravi H, Liu P, Peng SL, Liu H, Lu H. Simultaneous multi-slice (SMS) acquisition enhances the sensitivity of hemodynamic mapping using gas challenges. NMR in biomedicine 2016;29(11): 1511–8. [PubMed: 27598821]

[41]. Reinhard M, Schwarzer G, Briel M, Altamura C, Palazzo P, King A, et al. Cerebrovascular reactivity predicts stroke in high-grade carotid artery disease. Neurology 2014;83(16):1424–31. [PubMed: 25217057]

[42]. Nemoto EM, Snyder JV, Carroll RG, Morita H. Global ischemia in dogs: cerebrovascular CO2 reactivity and autoregulation. Stroke 1975;6(4):425–31. [PubMed: 1154479]

[43]. Dettmers C, Young A, Rommel T, Hartmann A, Weingart O, Baron JC. CO2 reactivity in the ischaemic core, penumbra, and normal tissue 6 hours after acute MCA-occlusion in primates. Acta neurochirurgica 1993;125(1-4):150–5. [PubMed: 8122541]

[44]. Olah L, Franke C, Schwindt W, Hoehn M. CO(2) reactivity measured by perfusion MRI during transient focal cerebral ischemia in rats. Stroke 2000;31(9):2236–44. [PubMed: 10978058]

[45]. Shih AYFB, Drew PJ, Tsai PS, Lyden PD, Kleinfeld D. Active dilation of penetrating arterioles restores red blood cell flux to penumbral neocortex after focal stroke. J Cereb Blo Flo Meta 2009;29:738–51.

[46]. Powers WJ, Press GA, Grubb RL Jr., Gado M, Raichle ME. The effect of hemodynamically significant carotid artery disease on the hemodynamic status of the cerebral circulation. Annals of internal medicine 1987;106(1):27–34. [PubMed: 3491558]

[47]. Nemoto EM, Yonas H, Kuwabara H, Pindzola RR, Sashin D, Meltzer CC, et al. Identification of hemodynamic compromise by cerebrovascular reserve and oxygen extraction fraction in occlusive vascular disease. Journal of cerebral blood flow and metabolism : official journal of the International Society of Cerebral Blood Flow and Metabolism 2004;24(10):1081–9.

[48]. Schlaug G, Siewert B, Benfield A, Edelman RR, Warach S. Time course of the apparent diffusion coefficient (ADC) abnormality in human stroke. Neurology 1997;49(1):113–9. [PubMed: 9222178]

[49]. Lansberg MG, Thijs VN, O'Brien MW, Ali JO, de Crespigny AJ, Tong DC, et al. Evolution of apparent diffusion coefficient, diffusion-weighted, and T2-weighted signal intensity of acute stroke. AJNR American journal of neuroradiology 2001;22(4):637–44. [PubMed: 11290470]

[50]. Liu P, Welch BG, Li Y, Gu H, King D, Yang Y, et al. Multiparametric imaging of brain hemodynamics and function using gas-inhalation MRI. Neuroimage 2017;146:715–23. [PubMed: 27693197]

[51]. Grandin CB, Duprez TP, Smith AM, Oppenheim C, Peeters A, Robert AR, et al. Which MR-derived perfusion parameters are the best predictors of infarct growth in hyperacute stroke? Comparative study between relative and quantitative measurements. Radiology 2002;223(2):361–70. [PubMed: 11997538]

[52]. Sobesky J, Zaro Weber O, Lehnhardt FG, Hesselmann V, Thiel A, Dohmen C, et al. Which time-to-peak threshold best identifies penumbral flow? A comparison of perfusion-weighted magnetic resonance imaging and positron emission tomography in acute ischemic stroke. Stroke 2004;35(12):2843–7. [PubMed: 15514190]

[53]. Lee M, Zaharchuk G, Guzman R, Achrol A, Bell-Stephens T, Steinberg GK. Quantitative hemodynamic studies in moyamoya disease: a review. Neurosurgical focus 2009;26(4):E5.

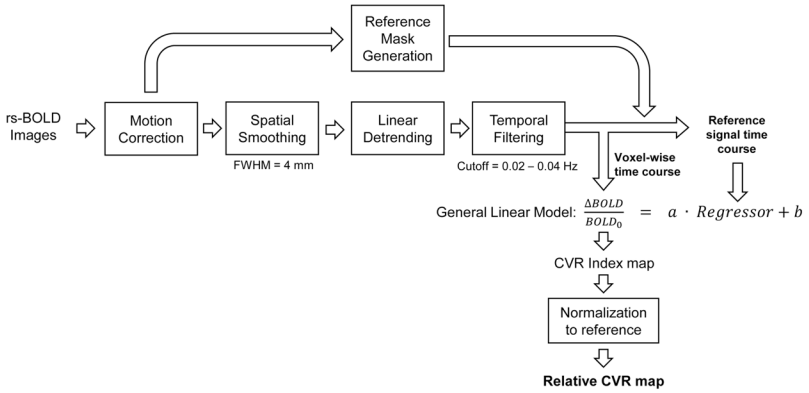

Figure 1:
Illustration of the analysis steps of relative CVR using resting-state BOLD MRI data.

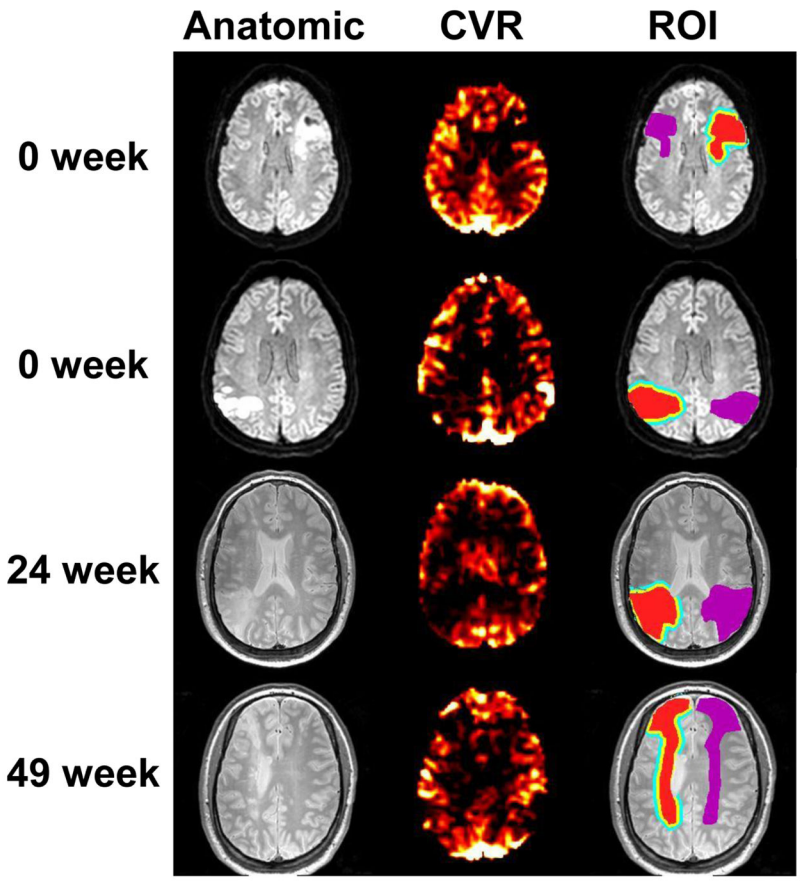

Figure 2:

Example images from four stroke patients. For each patient, the anatomic image (DWI or T2-weighted image), the relative CVR map, as well as the lesion/perilesional ROIs are shown. In the ROI images, the red areas indicate manually drawn lesion ROIs, the yellow areas represent the perilesion 1 ROIs, the blue areas represent the perilesion 2 ROIs, and the purple areas represent the control ROIs. Ventricle voxels are excluded from all ROIs.

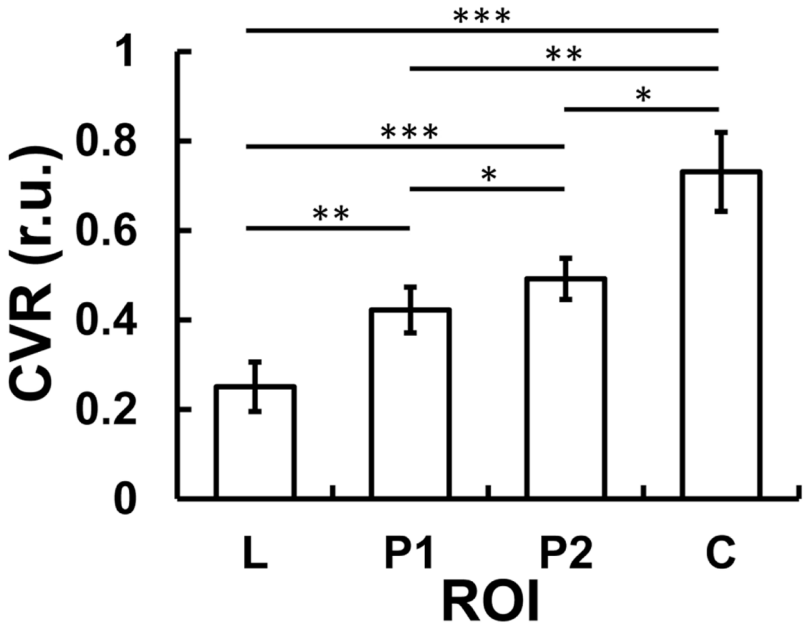

Figure 3:

Group-averaged relative CVR values from each ROI type in stroke patients. L, P1, P2, and C are abbreviations for lesion, perilesion 1, perilesion 2, and control, respectively. Error bars represent standard error. * indicates $p < 0.05$. ** indicates $p < 0.01$. *** indicates $p < 0.001$.

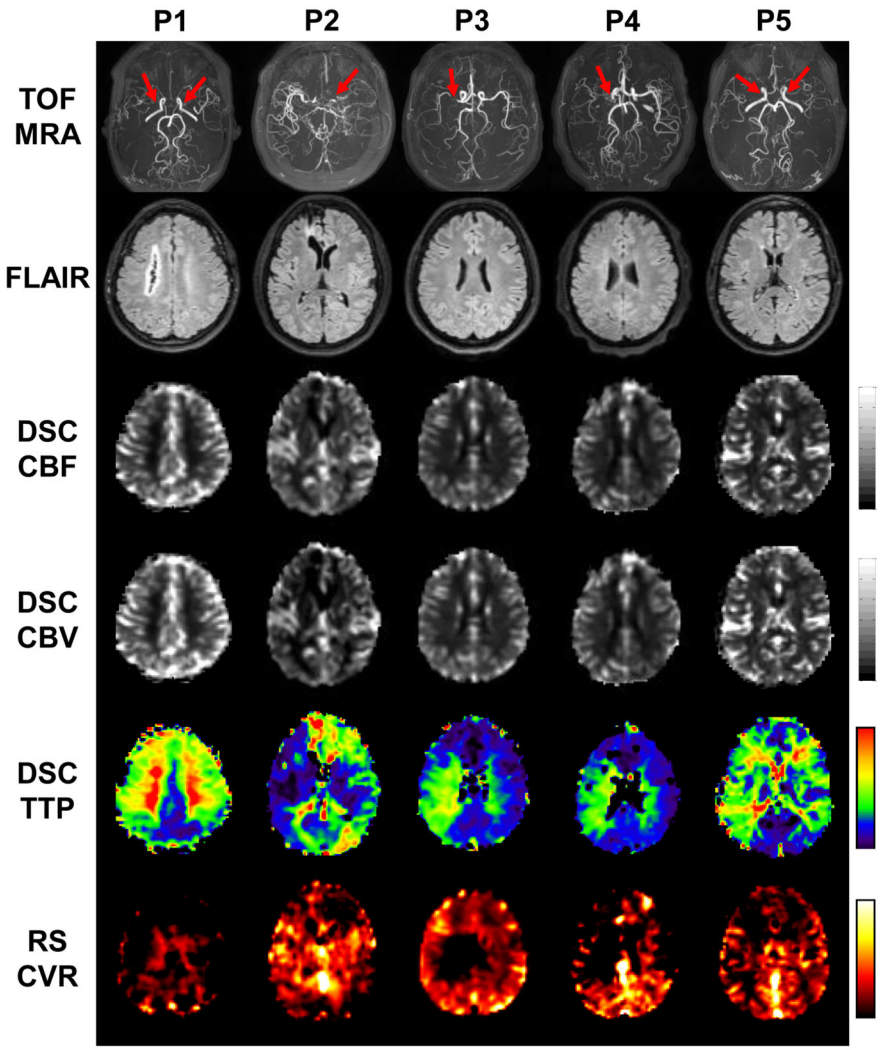

Figure 4:

Imaging results from the five patients with Moyamoya diseases. Row 1: Time-of-flight (TOF) MR angiograms (MRA). Red arrows indicate the sites of arterial stenosis. Row 2: T2-FLAIR images. Row 3: DSC-CBF maps. Row 4: DSC-CBV maps. Row 5: DSC-TTP maps. Row 6: rs-CVR maps.

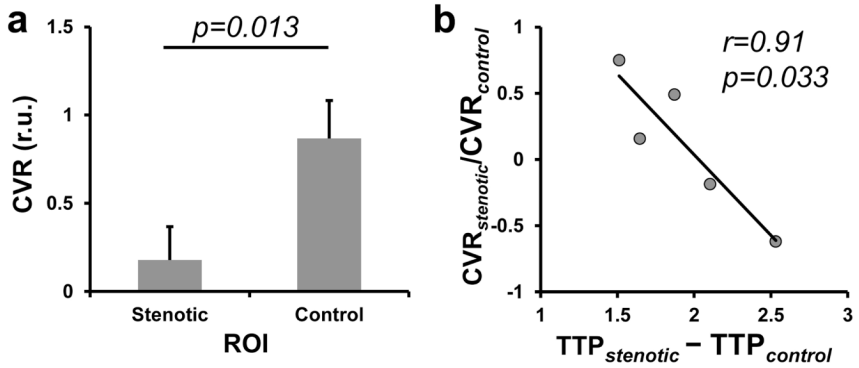

Figure 5.

Results of the ROI analysis in Moyamoya patients. (a) Comparison of relative CVR values between stenotic ROI and control ROIs. Error bars represent standard errors. (b) Scatter plot between CVR reduction and TTP lengthening in stenotic regions. Each dot represents data from one patient.

Table 1:

Demographic and Clinical Data of the stroke patients enrolled in this study.

Subject Number	Time of Scan Post-Stroke (Weeks)	Age	Sex	Race	NIHSS	Infarct Location
1	0	64	M	B	2	Right Cingulate Gyrus, Right Parieto-Occipital Lobe Junction, Left Parietal Lobe, Bilateral Occipital Lobes and Right Middle Cerebral Peduncle
2	0	52	M	A	1	Right Frontal Opercular Region
3	0	76	M	B	2	Right Temporal Lobe and Small Adjacent Gyral Infarctions in Right Anterior Occipital Lobe
4	0	66	M	W	2	Left Temporal Lobe and Left Parietal Lobe
5	0	57	F	B	2	Left Thalamus
6	1	39	F	Other	2	Left thalamus and Medial Aspect of the Left Midbrain
7	2	46	M	B	1	Left Thalamus
8	2	59	M	W	1	Gyrus with Extension to Deep White Matter and Basal Ganglia
9	7	63	M	W	0	Right Frontal Opercular Region and Temporal Lobe
10	11	71	F	W	2	Right Parieto-Occipital Lobe
11	20	54	F	B	3	Left Hemisphere
12	24	57	F	B	1	Right Hemisphere
13	24	56	M	W	2	Temporal lobe, Insular Region and Frontal Operculum/Inferior Lobe
14	32	46	F	W	9	Left Thalamus and Basal Ganglia
15	49	40	M	W	1	Sellar Mass with Suprasellar Extension
16	52	60	M		4	Right Hemisphere
17	52	49	M	B	0	Medial Left Occipital Lobe
18	52	65	M	B	1	Posterior Limb of the Right Internal Capsule with Extension to Basal Ganglia and Thalamus
19	59	54	M	B	2	Left Caudothalamic Groove/Genu of the Internal Capsule and Left Globus Pallidus
20	63	51	F	B	3	Left Hemisphere
Mean ± SD	22.50 ± 23.61	56.25 ± 9.70			2.05 ± 1.90	

Note: NIHSS: National Institutes of Health Stroke Scale. A: Asian. B: Black. W: White.

Table 2:

Demographic information of the Moyamoya patients.

Subject Number	Age	Sex	Race	Diagnosis	Treatment before MRI
1	34	F	W	Bilateral supraclinoid occlusions	Bilateral bypass
2	36	F	W	Right ICA/MCA and left ACA occlusion; Left MCA Narrowing; Bilateral distal (P2-P3) PCA occlusions.	Untreated
3	38	F	W	Left MCA occlusion	Untreated
4	18	F	W	Left ICA and MCA occlusions	Untreated
5	38	M	W	Bilateral MCA occlusions	Bilateral bypass